Image Enhancement for Breast Cancer Detection on Screening Mammography Using Deep Learning

2023 International Conference on Computer Science, Information Technology and Engineering (ICCoSITE) | 979-8-3503-2095-4/23/$31.00 ©2023 IEEE | DOI: 10.1109/ICCoSITE57641.2023.10127835

1st Muhammad Yusuf Kardawi
Department of Informatics
Institut Teknologi Sepuluh Nopember
Surabaya, Indonesia
my.kardawi@gmail.com

2nd Riyanarto Sarno
Department of Informatics
Institut Teknologi Sepuluh Nopember
Surabaya, Indonesia
riyanarto@if.its.ac.id

***Abstract*— Mammography offers the most efficient approach for detecting breast illnesses early. Nevertheless, Image enhancement to improve breast cancer detection is required since mammograms are low-contrast and noisy images, and typical diagnostic markers such as microcalcifications and masses are challenging to identify. Due to this issue, this paper evaluates the impact of image enhancement on the performance of the deep learning approach and conducts qualitative and quantitative testing of various deep learning models in breast cancer classification. This study uses Mini Digital Database for Screening Mammography (Mini-DDSM) breast dataset containing cancer and normal images. The mammography images are then improved using morphological erosion and enhanced using two image enhancement algorithms which are Unsharp Masking (UM) and High-Frequency Emphasis Filtering (HEF). Deep learning classification algorithms such as ResNet, DenseNet, and EfficientNet are employed to classify breast cancer. Each architecture is compared and analyzed regarding the effect of the image enhancement techniques and achieves the highest 76.08% accuracy score on breast cancer classification in the mammography dataset using the HEF technique.**

Keywords—image enhancement, deep learning, Unsharp Masking, High-Frequency Emphasis Filtering

I. INTRODUCTION

Breast cancer incidence was anticipated to reach 1.68 million in 2012, and it is likely to rise by 30% by 2025 [1]. Several countries have implemented mammography screening programs to aid in the early identification and therapy of bosom malignant growth to decrease mortality and other tragic outcomes. Mammography screening seems to affect mortality; randomized controlled preliminaries have shown a 20% decrease in bosom disease related passings subsequent to remembering mammography for bosom malignant growth screening [2], and a few nations have created public proposals or rules that recognize mammography for bosom malignant growth screening [3].

Many studies have established mammographic density, which is commonly defined in terms of the ratio of fibroglandular tissue to total breast area in mammography and referred to as percent density, as one of the most significant risk factors for breast cancer in women [4] [5]. Mammograms show fibroglandular (dense) tissue as a bright region, in contrast to the darker fat tissue and radiolucency portions. Several alternative techniques for calculating percent density have also been developed in recent years [6]-[9]. However, these devices run on the same principles. Although full-field digital mammography has essentially replaced screening film mammography, film mammography remains an important resource for breast density research since breast cancer is a latent illness, and film mammograms dating back 15 to 20 years contain evidence of numerous cancer outcomes. As a result, analyzing film mammograms will be crucial in furthering our understanding of breast cancer in the future.

Screening programs, as well as an increase in the number of breast cancer cases and treatments, have placed a significant burden on (breast) radiologists over the last two decades [10]. AI in computer-aided detection/diagnosis (CAD) systems assist radiologists while reducing effort. Classical CAD systems rely on traditional machine learning (ML) approaches, with predetermined characteristics (made by hand) sent into the system [11]. Extensive retrospective investigations, however, have demonstrated that typical CAD systems do not increase diagnosis accuracy [12].

Deep learning (DL), a subset of machine learning (ML), defines image data and specified features. Directly operates on image data, defining (learning) relevant attributes without human interaction. After the success of deep convolutional neural networks (CNNs) in 2012, substantial advances in computer vision have been made using DL [13]. Since then, deep learning techniques, notably CNN, have been quickly incorporated into medical image analysis [8] and employed in breast radiography to upgrade and improve conventional CAD systems to outperform radiological performance levels [14]. Also, many studies compared different neural network architectures [15]. DL is a new machine learning model that integrates many models produced from supervised and unsupervised learning techniques, resulting in improved outcomes. [16]. DL is utilized in a large number of utilizations and comprises more than one hidden layer. The fundamental benefit of DL is that it is a "structure freethinker" and that implies that no extraordinary suppositions should be made about the configuration of the contribution (for instance, the information should be an image, video, sound, or something different) [17]. However, one of the issues that has arisen as a result of machine learning is the curse of dimensionality, in which it struggles to manage large amounts of data input with a high dimension [18].

The primary goal of this study is to compare the effects of distinct pre-processing methods (UM [19] and HEF [20]) on the usage of pre-trained CNNs for breast cancer diagnosis. On medical images, the UM and HEF algorithms performed admirably [21] [22]. This approach opens the door for alternative, cutting-edge enhancing techniques to be considered before medical image categorization. As a result, we employ a broad technique as a foundation for this study and early work merging Mammography image improvement and deep learning models.

ResNet [23], DenseNet [24], and EfficientNet [25] architectures will be used as DL technique in this study due to their exceptional precision and sturdiness, notably in image classification, so they can recognize characteristics and patterns in the image, enabling works like identification and recognition to be performed. The most significant contributions to this research are:

- Analysis of the best type of image enhancement method for mammography images.
- Qualitative and quantitative testing of types of deep learning models in breast cancer classification after training improved image datasets using the UM and HEF algorithms, it is provided.
- Furthermore, various fine-tuned factors, especially enhancement parameters, are thoroughly explained.

II. MATERIAL AND METHOD

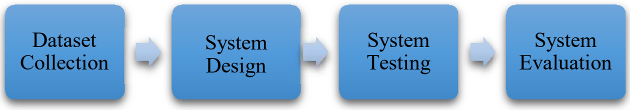

Fig. 1. Diagram for the implementation method

The first stage in developing a breast cancer classification system is collecting mammography data of normal and cancer-infected breasts from the Mini-DDSM dataset [26]. Table 1 shows the description of each class.

TABLE I. DESCRIPTION OF DATASET

Data type	Normal	Cancer	Total
Train Data	1.879	1892	3.771
Val Data	537	541	1.078
Test Data	268	270	538
Total	2.684	2.703	5.387

Each class differentiates between class levels, with the Normal class meaning negative mammography images and the Cancer class being positive mammography images.

A. System Design and Development

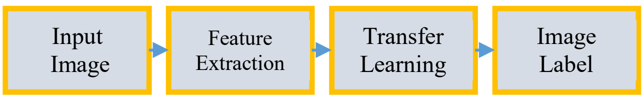

Fig. 2. The architecture for breast cancer detection

In this Section, there are several stages. First, the mammography image is entered into the system. The image is extracted from Low-level and High-level features, and the transfer learning process is carried out using ResNet [23], DenseNet [24], and EfficientNet [25] to produce normal or cancer labels.

Dataset Training Process

Initially, training the normal and cancer images is used. The suggested system has 2.684 photos with normal categories and 2.703 images with problematic types (infected cancer). The obtained datasets are then separated into two classes: normal mammography images and cancer mammography images.

The dataset is organized into three sections: 70% training, 20% validation, and 10% testing dataset. PyTorch Framework is used for training, validation, and testing. The CNN model is trained using three distinct architectures: ResNet50, DenseNet201, and Efficientnet-B4.

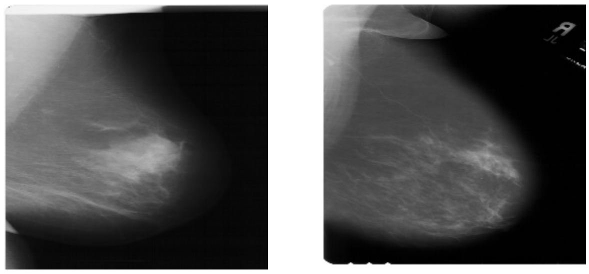

Fig. 3. Mammography dataset sample

B. Image Enhancement

Image-enhancing methods have increased image quality and accomplished the intended result [27]. Well-known image -enhancing procedures incorporate histogram evening out [28], low-pass separating, and high-pass sifting [29]. The essential objective of histogram evening out is to expand an visual impact of an image broadening the dark scale range of the image dissemination. This allows the approach to achieve its goal of increasing contras. As an outcome, the input image with many gray scales is synthesized into a single gray level, resulting in the loss of visual information. A high-pass or low-pass filter may only be used for image smoothing or sharpening [30].

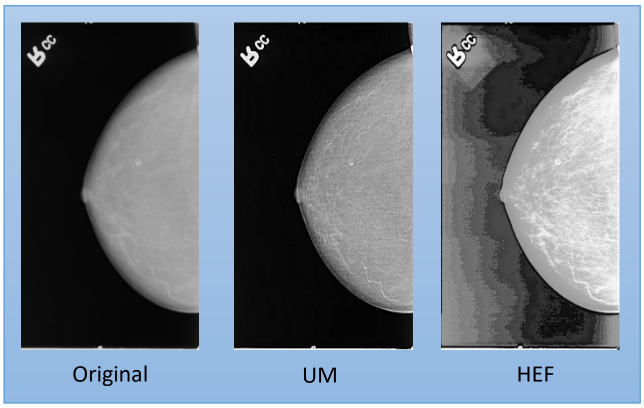

Fig. 4. Image comparison of standard mammography-enhanced UM and HEF images.

This work enhances the visibility of mammographic images before the DL classification stage by utilizing two effective image enhancement techniques, UM and HEF. Each approach is carried out and assessed separately.

Morphological Erosion

By decreasing the foreground, this approach employs erosion procedures to increase and improve image quality. On the other hand, the performance of morphological image processing is determined by the structural elements and image foreground qualities that must be recovered. Erosion is the fundamental activity of morphological image processing.

The erosion process reduces the foreground structure, and the shape of the structuring element impacts the performance of the operation. The background labels are removed using the erosion approach [31].

Unsharp Masking

Unsharp Masking [19] is a image -honing procedure that makes a cover of the first image by utilizing a mutilated, or "unsharp," negative image. To deliver a less fluffy image, the unsharp image is blended in with the first certain image. In other terms, UM is a linear filter that may enhance the image's high frequencies. The procedure begins with a duplicate of the original image and the application of a Gaussian blur. The radius setting is crucial for executing Gaussian blur. The radius is related to the blur intensity since it defines the size of the edges.

$$G(i, j) = \frac{1}{2\pi\sigma^2} e^{-\frac{i^2+j^2}{2\sigma^2}} \tag{1}$$

The distance from the origin is represented by i and j on the horizontal and vertical axes. It is also the standard deviation of the Gaussian appropriation. The obscured image is then extricated from the first image, abandoning just the fluffy edges. This is known as the "unsharp mask". Finally, the improved image is gathered after using the following equation:

$$I_{um\_enhanced} = I_{ori} + \text{amount} * (I_u) \tag{2}$$

$I_{um\_enhanced}$, I_{ori}, and I_u is the final UM algorithm results, the original image, and the unsharp image, respectively. The radius and quantity (in Eq. (2)) are discussed in further detail below:

- Amount relates to how much difference is supplied to the border (how much the brightness).
- Radius impacts the length of the enhanced edge or how prominent the edge is. Therefore, a lower radius improves the accuracy of a smaller scale.

There are several standards for the initial value of this option, and its relevance varies from implementation to implementation [32].

High-frequency Emphasis Filtering

HEF [20] is a method for emphasizing and highlighting edges that employ a Gaussian high-pass filter. Edges are often depicted in the high-frequency spectrum due to their more dramatic intensity fluctuations. Histogram equalization is required to boost ratio and clarity in images produced by this technology. This technique's filter step employs a Gaussian high-pass filter (the strength of which is governed by the radius setting) (see equation (3)). To get the filter function, the image must be sent through the Fourier transform, as shown in equation (4). Following the inverse transformation (see equation (5)), we will obtain the filtered image. Figure 5 depicts the steps of the HEF approach. [32].

$$G\_Filter(i, j) = 1 - e^{-D^2(i,j)/2D_0^2} \tag{3}$$

Where D_0 is the cutting distance. The Fourier transform of f(x,y), denoted by F(i,j), for x and i = 0,1,2......M - 1 and y and j = 0,1,2.....N - 1, as determined by the formula:

$$F(i, j) = \sum_{x=0}^{M-1} \sum_{y=0}^{N-1} f(x, y) e^{-j2\pi(\frac{ix}{M}+\frac{jy}{N})} \tag{4}$$

Here is the formula for the inverse Fourier transform:

$$F(x, y) = \frac{1}{MN} \sum_{i=0}^{M-1} \sum_{j=0}^{N-1} f(i, j) e^{-j2\pi(\frac{ix}{M}+\frac{jy}{N})} \tag{5}$$

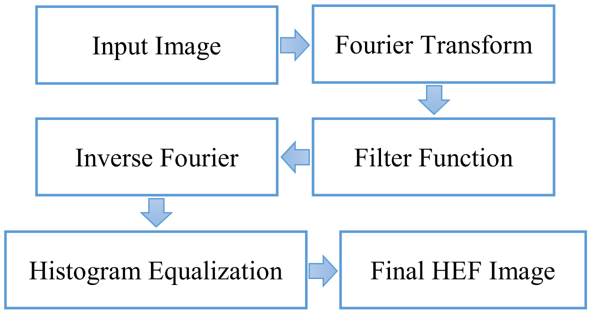

Fig. 5. Using Fourier-domain filtering to apply HEF.

Finally, the image contrast is adjusted by simple histogram equalization (Hist_Eq):

$$I_{hef\_sharpened} = (I_{ori} + (G\_Filter)) * (Hist\_Eq) \tag{6}$$

C. Breast Cancer Classification Development

Mammography images pre-processed with morphological erosion and image enhancement UM and HEF will be used as input images in the breast cancer diagnosis stage. The input to CNN is considered to be an image. This approach allows specific network attributes to be encoded. Due to the binary nature of the study's input, the pixels would be arranged in height, width, and depth (e.g., 224x224x3).

TABLE II. DATA TRAINING PARAMETER

Parameter	ResNet	VggNet	EfficientNet
Optimizer	SGD	SGD	SGD
Epoch	30	30	30
Batch Size	6	6	6
Learning rate (LR)	0.01	0.01	0.01
LR decay	0.5	0.5	0.5
LR step size	3	3	3
Weight decay	$1x10^{-5}$	$1x10^{-5}$	$1x10^{-5}$
Num of workers	10	10	10

Favorable characteristics may be extracted from image data by changing particular parameters in the convolution layer during training. In a fully connected layer, the parameter set is simultaneously learnt while categorizing the target class attributes (negative or positive images). The convolution layer extracts visual characteristics from the raw

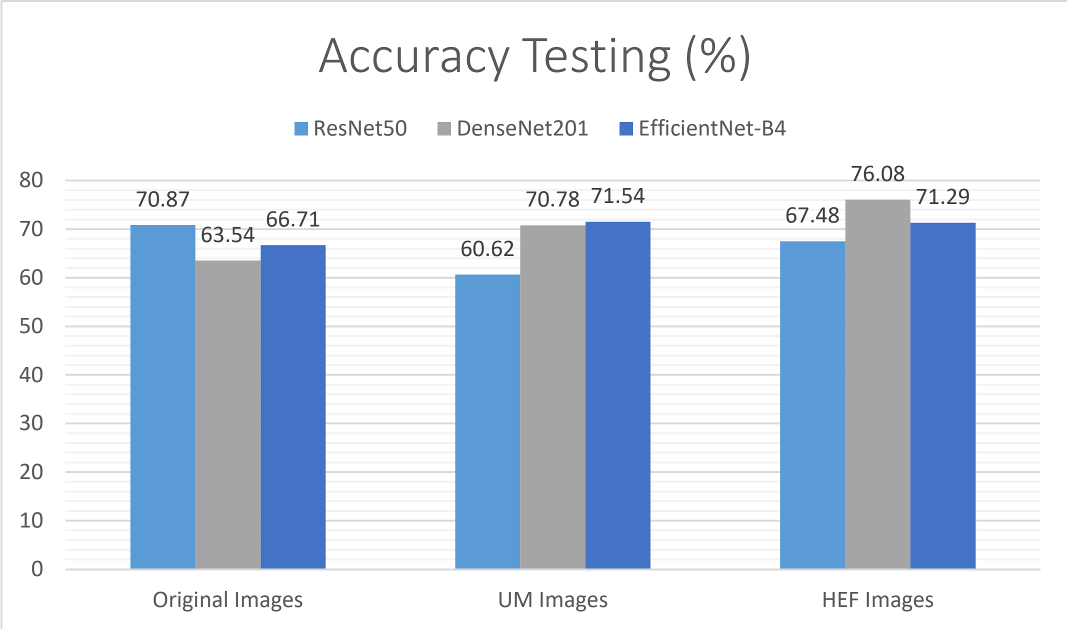

Fig. 6. Comparison of testing accuracy

input image in a hierarchical manner. Lower levels provide low-level visual components such as shapes or borders, and higher layers produce high-level visual aspects such as objects. Vectors are labels for images. In this case, the label is binary, with a value of '1' for a cancer image and a value of '0' for any other image [32].

In table II describes the parameters used in the training stage. Each model type has the same parameter configuration with Focal Loss as the error function used during the training process.

D. System Evaluation and Analysis

The last stage involves evaluating the system's capacity to classify breast cancer using the CNN technique on the ResNet, DenseNet, and EfficientNet designs. If the system's output is unsatisfactory, it is essential to enhance the system.

The accuracy of breast cancer identification will be tested and assessed at this stage. Each form of CNN architecture is examined to determine the accuracy of breast cancer detection prediction, and then the relevant architecture detection is explained. The system is considered complete if each design identifies breast cancer with an average accuracy better than 78%. Similarly, if the average accuracy rate is less than 70%, the causal variables impacting the accuracy rate in diagnosing breast cancer are studied. The study's findings will then be utilized and re-implemented to enhance the system as a reference in reaching a conclusion.

III. RESULTS AND DISCUSSION

The system that has been developed produces an accuracy score for each type of image that has been done training and inference on each split dataset. The output of this study produces a model that can classify between normal and cancer mammography images to increase the detection of breast cancer in screening mammography. The primary purpose of image quality improvement is to overcome the problems commonly experienced in screening mammography, namely in the form of low contrast and a lot of noise. In this paper, we perform morphological erosion to remove noisy mammography images and then pre-process the images by using contrast adjustment algorithms such as UM and HEF to overcome the previous low contrast problem. After various experiments, fig. 6 shows significant results regarding the effect of the multiple stages we proposed. Each type of architecture experienced an increase in the accuracy testing value after we applied image enhancement, especially the HEF algorithm.

The accuracy testing results indicate that the score obtained is very competitive. In images that have been applied UM techniques, DenseNet and EfficientNet architectures show relatively similar accuracy values. In this study, we gave the parameter values Radius: 6 and Amount: 2, which are the best parameters in our dataset. Also, we used D0: 40 as a parameter in the HEF technique. The higher the parameter value, the brighter the luminance level in the input image. The HEF enhancement technique gives the highest score on the DenseNet architecture and is the best accuracy value in this study.

In this research, the value we obtained is still below 80% because we only used the morphological operation stage before performing the image enhancement stage, which is the focus of our analysis. Other stages, such as removing white borders, removing artifacts and pectoral muscles, annotation, augmentation, and data distribution, can be applied to improve testing accuracy.

This study used ResNet50, DenseNet201, and EfficientNet-B4. In fig. 6, it can be seen that the performance of ResNet50 decreases in the accuracy testing value. In the original image, the ResNet architecture can provide an accuracy testing value of 70.87%, which is a better value than images that have undergone morphological erosion and image quality improvement with UM or HEF. ResNet [23] is a neural network that skips levels by using connections. Skipping layers prevents fading gradients by repeating the activation of the preceding layer before its surrounding layers know its weight. The depth of the architecture influences the effectiveness of the features extracted on the network. ResNet is built up of several layers, each of which is usually injected multiple times. In the ResNet-50 architecture, In the 34-layer network, a 3-layer congestion block is used to replace each 2-layer block [33]. The advantage of adding this type of skip connection is that if layers interfere with the architecture's performance of the architecture, then those layers will be skipped by the regularization. So, this results in training an intense neural network without the problems caused by vanishing/exploding gradients. However, in this experiment, skipping layers does not work well on images that have been enhanced because the skip connection connects the activation of a layer to further layers by skipping some of the layers in between. This forms residual blocks. The ResNet is created by stacking these residual blocks together. The approach behind this network is that instead of layers learning the underlying mapping, we allow the network to fit the residual mapping.

A. *Original Images*

Table III shows the comparison of training and validation values of each model on the original mammography images. The results explain that although the ResNet50 model has a poor validation loss score, it provides the highest training and validation accuracy values of 99.63% and 73.01%.

TABLE III. COMPARISON OF ORIGINAL IMAGES

Model	ResNet (%)	DenseNet (%)	EfficientNet (%)
Training Loss	00.49	02.96	03.52
Validation Loss	42.48	29.80	23.80
Train Accuracy	**99.63**	95.86	95.23
Validation Accuracy	**73.01**	69.67	72.73

B. *UM Images*

Unlike the original images, on mammography images with UM image enhancement, the EfficienNet-B4 model works better than other models. This is because EfficientNet-B4 has more layers and fewer parameters, resulting in more efficient architecture performance. EfficientNet [18] is a set of models generated from a base network, notably EfficientNet-B0 through B7 (called EfficientNet-B0). EfficientNet's benefits are stated in two ways. Model performance is improved by lowering parameters and flops (floating-point operations per second) [33]. The training and validation accuracy scores obtained are 99.89% and 75.05%. The validation accuracy value is the highest for each type of mammography image.

TABLE IV. COMPARISON OF UM IMAGES

Model	ResNet (%)	DenseNet (%)	EfficientNet (%)
Training Loss	00.35	00.64	00.70
Validation Loss	38.26	33.22	90.78
Train Accuracy	99.66	99.28	**99.89**
Validation Accuracy	73.28	74.49	**75.05**

C. *HEF Images*

The last test result using HEF images. This dataset gives different results, with the ResNet50 model getting the best train accuracy score and the EfficientNet-B4 model giving the highest validation score. The Train Accuracy Score on the ResNet50 model is the highest value for each image type.

TABLE IV. COMPARISON OF HEF IMAGES

Model	ResNet (%)	DenseNet (%)	EfficientNet (%)
Training Loss	00.11	00.20	00.59
Validation Loss	39.85	50.06	103.1
Train Accuracy	**99.95**	99.84	99.87
Validation Accuracy	71.89	68.92	**73.28**

A breakdown of each model in test data results from each type of image can be seen in fig. 6, and the diagram shows the test accuracy score of each model obtained in this study. Overall, the DenseNet201 model provides the best accuracy score of 76.08%, and the model with images enhanced through UM and HEF provides a higher accuracy score than the original image.

IV. CONCLUSION

This paper uses ResNet50, DenseNet201, and efficientNet-B4 architectures to train mammography images and improve detection accuracy by combining DL techniques with Unsharp Masking (UM) and High-Frequency Emphasis Filtering (HEF). Experiments show that the accuracy of the idea is very competitive. It revealed that each architecture provides the best test accuracy for each image enhancement technique, namely 70.87% on original images (ResNet50 architecture), 71.54% on UM images (EfficientNet-B4 architecture), and the highest score of 76.08% with HEF images (DenseNet201 architecture). Furthermore, the overall mammography images enhanced through UM and HEF techniques give a better detection accuracy score than mammography images without image enhancement. As a pre-processing on breast mammography images, the image enhancement system will help the tested pre-trained network understand the model better. More image-enhancing approaches will be evaluated in the future to demonstrate more substantial effects on DL models. Furthermore, complete subjective opinions and preferences from medical specialists will be examined.

ACKNOWLEDGMENT

This research was funded by Lembaga Pengelola Dana Pendidikan (LPDP) under Riset Inovatif-Produktif (RISPRO) Program; the Indonesian Ministry of Education and Culture under Penelitian Terapan Unggulan Perguruan Tinggi (PTUPT) Program; and Institut Teknologi Sepuluh

Nopember (ITS) under project scheme of the Publication Writing and IPR Incentive Program (PPHKI).

REFERENCES

[1] B. L. Secretan, D. Ph, C. Scoccianti, D. Ph, D. Loomis, and D. Ph, “Special Report Breast-Cancer Screening — Viewpoint of the IARC Working Group,” pp. 2353–2358, 2015.

[2] Myers ER, Moorman P, Gierisch JM, Havrilesky LJ, Grimm LJ, Ghate S, et al. Benefits and harms of breast cancer screening: a systematic review. JAMA 2015;314:1615-1634

[3] J. H. Yoon and E. K. Kim, “Deep learning-based artificial intelligence for mammography,” Korean J. Radiol., vol. 22, no. 8, pp. 1225–1239, 2021, doi: 10.3348/KJR.2020.1210.

[4] M. N. Linver, “4-19 Mammographic Density and the Risk and Detection of Breast Cancer,” Breast Dis., vol. 18, no. 4, pp. 364–365, 2008, doi: 10.1016/S1043-321X(07)80400-0.

[5] I. Schreer, “Dense breast tissue as an important risk factor for breast cancer and implications for early detection,” Breast Care, vol. 4, no. 2, pp. 89–92, 2009, doi: 10.1159/000211954.

[6] J. Li et al., “High-throughput mammographic-density measurement: a tool for risk prediction of breast cancer,” Breast Cancer Res., vol. 14, no. 4, 2012, doi: 10.1186/bcr3238.

[7] I. dos S. S. Valerie A. McCormack, Ralph Highnam, Nicholas Perry, “Europe PMC Funders Group Comparison of a New and Existing Method of Mammographic Density Measurement :,” vol. 16, no. 6, pp. 1148–1154, 2009, doi: 10.1158/1055-9965.EPI-07-0085.Comparison.

[8] J. A. Shepherd, K. M. Kerlikowske, R. Smith-Bindman, H. K. Genant, and S. R. Cummings, “Measurement of breast density with dual X-ray absorptiometry: Feasibility,” Radiology, vol. 223, no. 2, pp. 554–557, 2002, doi: 10.1148/radiol.2232010482.

[9] J. J. Heine et al., “An automated approach for estimation of breast density,” Cancer Epidemiol. Biomarkers Prev., vol. 17, no. 11, pp. 3090–3097, 2008, doi: 10.1158/1055-9965.EPI-08-0170.

[10] Wing P, Langelier MH: Workforce shortages in breast imaging: impact on mammography utilization. Am J Roentgenol 192(2):370-378, 2009. https://doi.org/10.2214/AJR.08.1665

[11] Litjens G, Kooi T, Bejnordi BE, et al: A survey on deep learning in medical image analysis. Med Image Anal 42:60-88, 2017. https://doi.org/10.1016/j.media.2017.07.005

[12] Lehman CD, Wellman RD, Buist DSM, et al: Diagnostic accuracy of digital screening mammography with and without computer-aided detection. JAMA Inter Med 175(11):1828-1837, 2015. https://doi.org/10.1001/jamainternmed.2015.5231

[13] Krizhevsky, A., Sutskever, I., & Hinton, G.E. "ImageNet classification with deep convolutional neural networks," Communications of the ACM, 2012, 60, 84 - 90.

[14] L. Balkenende, J. Teuwen, and R. M. Mann, “Application of Deep Learning in Breast Cancer Imaging,” Semin. Nucl. Med., vol. 52, no. 5, pp. 584–596, 2022, doi: 10.1053/j.semnuclmed.2022.02.003.

[15] R. Sarno, J. Sidabutar, and Sarwosri, “Comparison of different Neural Network architectures for software cost estimation,” Proceeding - 2015 Int. Conf. Comput. Control. Informatics Its Appl. Emerg. Trends Era Internet Things, IC3INA 2015, pp. 68–73, 2016, doi: 10.1109/IC3INA.2015.7377748.

[16] R. Sarno, S. I. Sabilla, and D. Rahmanwijaya, “Electronic Nose for Detecting Multilevel Diabetes using Optimized Deep Neural Network,” Eng. Lett., vol. 28, no. 1, pp. 31–42, 2020.

[17] Malikhah et al., “Detection of Infectious Respiratory Disease Through Sweat From Axillary Using an E-Nose With Stacked Deep Neural Network,” IEEE Access, vol. 10, pp. 51285–51298, 2022, doi: 10.1109/ACCESS.2022.3173736.

[18] S. I. Sabilla, R. Sarno, K. Triyana, and K. Hayashi, “Deep learning in a sensor array system based on the distribution of volatile compounds from meat cuts using GC–MS analysis,” Sens. Bio-Sensing Res., vol. 29, no. July, p. 100371, 2020, doi: 10.1016/j.sbsr.2020.100371.

[19] A. Polesel, G. Ramponi, and V. J. Mathews, ‘‘Image enhancement via adaptive unsharp masking,’’ IEEE Trans. Image Process., vol. 9, no. 3, pp. 505–510, Mar. 2000.

[20] A. Bundy and L. Wallen, ‘‘High-emphasis filtering,’’ in Catalogue of Artificial Intelligence Tools. Berlin, Germany: Springer, 1984, p. 47.

[21] A. Wubuli, J. Zhen-Hong, Q. Xi-Zhong, Y. Jie, and N. Kasabov, ‘‘Medical image enhancement based on shearlet transform and unsharp masking,’’ J. Med. Imag. Health Informat., vol. 4, no. 5, pp. 814–818, Oct. 2014.

[22] K. Panetta, Y. Zhou, S. Agaian, and H. Jia, ‘‘Nonlinear unsharp masking for mammogram enhancement,’’ IEEE Trans. Inf. Technol. Biomed., vol. 15, no. 6, pp. 918–928, Nov. 2011.

[23] J. S. K. He, X. Zhang, S. Ren, "Deep Residual Learning for Image Recognition," IEEE Conf. Comput. Vis. Pattern Recognit., pp. 770–778, 2016, doi:10.1002/chin.200650130.

[24] G. Huang, Z. Liu, L. Van Der Maaten and K. Q. Weinberger, "Densely Connected Convolutional Networks," 2017 IEEE Conference on Computer Vision and Pattern Recognition (CVPR), 2017, pp. 2261-2269, doi: 10.1109/CVPR.2017.243.

[25] M. Tan and Q. V. Le, "EfficientNet: Rethinking model scaling for convolutional neural networks," 36th Int. Conf. Mach. Learn. ICML 2019, vol. 2019- June, pp. 10691–10700, 2019.

[26] C. D. Lekamlage, F. Afzal, E. Westerberg, and A. Chaddad, “Mini-DDSM: Mammography-based Automatic Age Estimation,” ACM Int. Conf. Proceeding Ser., no. Dmip 2020, pp. 1–6, 2020, doi: 10.1145/3441369.3441370.

[27] A. Wubuli, J. Zhen-Hong, Q. Xi-Zhong, Y. Jie, and N. Kasabov, ‘‘Medical image enhancement based on shearlet transform and unsharp masking,’’ J. Med. Imag. Health Informat., vol. 4, no. 5, pp. 814–818, Oct. 2014.

[28] A. M. Reza, ‘‘Realization of the contrast limited adaptive histogram equalization (CLAHE) for real-time image enhancement,’’ J. VLSI signal Process. Syst. signal, image video Technol., vol. 38, no. 1, pp. 35–44, 2004.

[29] S. S. Agaian, K. Panetta, and A. M. Grigoryan, ‘‘Transform-based image enhancement algorithms with performance measure,’’ IEEE Trans. Image Process., vol. 10, no. 3, pp. 367–382, Mar. 2001.

[30] A. Bundy and L. Wallen, ‘‘High-emphasis filtering,’’ in Catalogue of Artificial Intelligence Tools. Berlin, Germany: Springer, 1984, p. 47.

[31] K. A. M. Said and A. B. Jambek, “Analysis of Image Processing Using Morphological Erosion and Dilation,” J. Phys. Conf. Ser., vol. 2071, no. 1, 2021, doi: 10.1088/1742-6596/2071/1/012033.

[32] K. Munadi, K. Muchtar, N. Maulina and B. Pradhan, "Image Enhancement for Tuberculosis Detection Using Deep Learning," in IEEE Access, vol. 8, pp. 217897-217907, 2020, doi: 10.1109/ACCESS.2020.3041867.

[33] M. Y. Kardawi, K. Muchtar, Y. Nurdin, N. Maulina and S. Muchallil, "A Comparative Analysis of Deep Learning Models for Detection of Knee Osteoarthritis Disease through Mobile Apps," 2022 8th International Conference on Wireless and Telematics (ICWT), 2022, pp. 1-6, doi: 10.1109/ICWT55831.2022.9935417.